The phase behavior of linear and partially flexible hard-sphere chain fluids and the solubility of hard spheres in hard-sphere chain fluids

Bernardo Oyarzún, Thijs van Westen, and Thijs J. H. Vlugt[a)]
Process and Energy Laboratory, Delft University of Technology, Delft, The Netherlands

(Received 19 March 2013; accepted 3 May 2013; published online 24 May 2013)

The liquid crystal phase behavior of linear and partially flexible hard-sphere chain fluids and the solubility of hard spheres in hard-sphere chain fluids are studied by constant pressure Monte Carlo simulations. An extensive study on the phase behavior of linear fluids with a length of 7, 8, 9, 10, 11, 12, 13, 14, 15, and 20 beads is carried out. The phase behavior of partially flexible fluids with a total length of 8, 10, 14, and 15 beads and with different lengths for the linear part is also determined. A precise description of the reduced pressure and of the packing fraction change at the isotropic-nematic coexistence was achieved by performing long simulation runs. For linear fluids, a maximum in the isotropic to nematic packing fraction change is observed for a chain length of 15 beads. The infinite dilution solubility of hard spheres in linear and partially flexible hard-sphere chain fluids is calculated by the Widom test-particle insertion method. To identify the effect of chain connectivity and molecular anisotropy on free volume, solubility is expressed relative to that of hard spheres in a hard sphere fluid at same packing fraction as relative Henry's law constants. A linear relationship between relative Henry's law constants and packing fraction is observed for all linear fluids. Furthermore, this linearity is independent of liquid crystal ordering and seems to be independent of chain length for linear chains of 10 beads and longer. The same linear relationship was observed for the solubility of hard spheres in nematic forming partially flexible fluids for packing fractions up to a value slightly higher than the nematic packing fraction at the isotropic-nematic coexistence. At higher packing fractions, the small flexibility of these fluids seems to improve solubility in comparison with the linear fluids. © *2013 AIP Publishing LLC*. [http://dx.doi.org/10.1063/1.4807056]

I. INTRODUCTION

Liquid crystals are condensed phases whose molecular constituents are arranged with a partial order between the liquid and crystal states. Liquid crystal phases are classified depending on the orientational and positional distribution of molecules. In the isotropic (*Iso*) phase, molecules are distributed isotropically without any long-range orientational or positional order.[1] In the nematic (*Nem*) phase, molecules show no positional ordering but are distributed around a preferred axis of orientation. The unit vector that identifies this preferred orientation is known as the nematic director (**n**). In smectic phases, molecules do not only follow a preferred orientation but also have positional order forming molecular layers. In the smectic-A (*SmA*) phase, the nematic director and the normal vector of the smectic layer lay in parallel directions. In the smectic-C (*SmC*) phase, the nematic director is tilted with respect to the normal layer vector.

Liquid crystal molecules have an elongated shape with a typical structure formed by a rigid core with terminal substituents attached at its ends.[2] The rigid core is typically constituted by two or more (adjacent or linked) phenyl rings and the terminal substituents vary from mono-atomic groups to long flexible alkyl chains. The molecular order of liquid crystal phases and the anisotropic shape of liquid crystal molecules confer specific physical properties to liquid crystal fluids. For instance, circularly birefringence of twisted nematic liquid crystals is widely used for modulating light polarization in visual display devices.[3] Of particular interest is the solubility of gases in liquid crystals and their use as solvents for gas separation applications.[4] It has been shown that liquid crystals are able to absorb CO_2 in the isotropic phase and release it by cooling from the nematic phase.[5,6] These properties are of interest for improving the efficiency of CO_2 capture processes compared to the conventional amine-based process.[7]

It is generally understood that a certain degree of shape anisotropy is a necessary molecular attribute required for the emergence of liquid crystal phases.[1] More specifically, it is well known that anisotropic repulsive interactions only are sufficient for the formation of liquid crystal phases. This was first predicted theoretically by Onsager[8] and observed later in molecular simulation studies of hard disks,[9,10] hard ellipsoids,[11–14] hard spherocylinders,[15–20] and cut hard spheres.[21] Frenkel,[22] Allen,[23] Care and Cleaver,[24] and Wilson[25] provided excellent reviews on the molecular simulation of liquid crystals.

Hard-spheres are the simplest generic blocks that can be used for building molecular models in molecular simulations. In this context, linear hard-sphere chain molecules are the basic hard-sphere model to study liquid crystal phases. Vega *et al.*[26] studied the phase behavior of linear hard-sphere chain fluids with a length of 3, 4, 5, 6, and 7 beads from constant pressure Monte Carlo simulations. These authors observed

a)Electronic mail: t.j.h.vlugt@tudelft.nl

that hard-sphere chain fluids with a length of 5 beads and higher are able to form liquid crystal phases, while shorter chains experience a direct transition from the isotropic to the crystal state.[26–28] Williamson and Jackson[29] investigated the phase behavior of the 7 bead linear hard-sphere chain from the isotropic to the crystal state in more detail. The isotropic-nematic phase behavior of the 8 linear and of the 20 linear hard-sphere chain was obtained by Yethiraj and Fynewever.[30] Whittle and Masters[31] studied the phase behavior of 6 and 8 bead linear fused hard-sphere molecules with length-to-width ratios ranging from 3.5 to 5.2, observing a nematic phase only for the longest molecule. In this study, we investigate the liquid crystal phase behavior of linear hard-sphere chain fluids with lengths of 7–15 and 20 beads. In contrast with previous studies, the extensive collection of data obtained for these fluids allows us to accurately determine the isotropic-nematic phase transition.

Real liquid crystal molecules have a certain degree of flexibility which is mainly provided by alkyl terminal substituents.[2] It has been shown that increasing the flexibility of a molecule destabilizes the nematic and smectic phases favoring the isotropic state.[32,33] Introducing molecular flexibility into hard-sphere chain molecules can be done either homogeneously by semi-flexible molecules where a bond-bending and torsional potential is defined for the whole molecule, or heterogeneously by partially flexible molecules where potentials are defined for different parts of the molecule. The first approach was used by Wilson and Allen[32,34] for a 7 bead semi-flexible molecule bonded by potential wells, as well as by Yethiraj and Fynewever[30] who determined the isotropic and nematic phase behavior of 8 and 20 beads semi-flexible molecules with bending potentials of varying stiffness. A partially flexible model was employed by McBride and Vega *et al.*[33,35] for fused hard-sphere molecules composed of a linear and a freely jointed part with a total length of 15 beads and with 8–15 beads in the linear part. Escobedo and de Pablo[36] used the expanded Gibbs ensemble and the pseudo-Gibbs ensemble for calculating the isotropic-nematic phase transition of 8 and 16 hard-sphere chain molecules with finite and infinite bond bending potentials (linear chains). In this work, we use a partially flexible model formed by a linear and a freely jointed part, for investigating the effect of flexibility on the phase behavior of hard-sphere chain fluids and on the solubility of hard spheres in hard-sphere chain fluids. The linear hard-sphere chain model can be considered as a special case of the partially flexible model made of a linear part only.

A step change in the solubility of gases between the isotropic, nematic, and smectic phases has been observed in experiments.[5,6,37,38] It has been argued that free volume and molecular ordering are the driving forces behind this solubility difference.[37] Studies on the solubility of gases in ionic liquids solvents have shown that free volume is a fundamental solvent property behind the solubility of gases.[39,40] Free volume is related to the available volume for a molecule in a fluid and it is formally defined as the difference between the total and the excluded volume, $V_{\text{free}} = V - V_{\text{ex}}$, where the excluded volume V_{ex} is the volume that is not accessible for the center of mass of a molecule due to the presence of all other molecules in the fluid.[41] The magnitude of the excluded volume is related to the packing fraction, molecular configuration, and orientation of molecules in the fluid.[42,43] The relative effect of these factors on the free volume and, therefore, on the solubility of gases in liquid crystal solvents cannot be known *a priori*. We studied the infinite dilution solubility of hard spheres in linear and in partially flexible hard-sphere chain molecules with different flexibilities in the isotropic and nematic phases. Solubility is expressed in terms of Henry's law constants calculated from the chemical potential of hard spheres in hard-sphere chain fluids at infinite dilution.[44]

This paper is organized as follows. In Sec. II, we present details of the Monte Carlo simulation technique. In Sec. III, simulation results are presented for the phase behavior of, linear hard-sphere chain fluids (Sec. III A), the phase behavior of partially flexible hard-sphere chain fluids (Sec. III B), and the infinite dilution solubility of hard spheres in hard-sphere chain fluids (Sec. III C). Our results are summarized in Sec. IV.

II. MODEL AND SIMULATION METHODS

In this work, we use a partially flexible model consisting of a hard-sphere chain molecule formed by a linear and a freely jointed part.[43] The freely jointed part does not have any bond-bending or torsional potential; therefore, it is free to move between any possible molecular configuration limited only by a rigid bond length constraint and the infinite repulsion among hard-sphere beads. Partially flexible hard-sphere chain molecules are identified by the notation $m - m_r$ where m is the total length of the chain, and m_r is the total length of the rigid part. Linear hard-sphere chain molecules are identified by their total length m.

The phase behavior of linear and partially flexible hard-sphere chain fluids was obtained by Monte Carlo simulations in the isobaric-isothermal *NPT* ensemble. Periodic boundary conditions were used in a rectangular simulation box with varying orthogonal dimensions. The following Monte Carlo trial moves were used: displacement, rotation, volume change, and partial-regrowth of the freely jointed part using the configurational-bias Monte Carlo method.[45–48] In the configurational-bias Monte Carlo method, 10 trail directions were attempted for regrowing each bead in the freely jointed part. A system size of $N = 350$ molecules was used for all simulations except for the 7 and 8 linear tangent hard-sphere chain fluids in which a larger number of 576 molecules was employed. The latter was done in order to compare actual simulation results with previous simulation data, especially with that obtained by Williamson and Jackson[29] for the 7 linear hard-sphere fluid. Simulations with 216 and 350 molecules were also performed for the 7 linear fluid in order to study the system size effect. In the equilibration period, the maximum displacement and rotation angle were adjusted in order to obtain an acceptance ratio of 20%. Rotation around every Cartesian axes was considered separately due to the orientation of molecules around the nematic director in nematic and smectic phases. Volume changes were performed in an anisotropic manner by choosing independently the box side which is expanded/contracted.[30,33] In this way, the natural anisotropy introduced by a rectangular box is decoupled

from the phase anisotropy inherent to ordered systems. Displacement and rotation trial moves were selected with the same probability, while the probability of attempting a volume change was set to 2%. In the case of partially flexible molecules, 15% of the trial moves were attempted to regrow the freely jointed part. The anisotropic expansion of the simulation box may result in the contraction of one of its dimensions to zero due to the finite size of the system. This event is avoided by using large system sizes but at the cost of long simulation runs. A good balance between a very low occurrence of this event and short simulation runs was obtained for a system size of 350 molecules. A typical simulation run comprises 1×10^6 Monte Carlo cycles in the equilibration period and 1×10^6 cycles in the production period. Every Monte Carlo cycle consisted of a total of N Monte Carlo trial moves. However, close to the isotropic-nematic transition region, the required number of simulation cycles in the equilibration and production periods was normally doubled due to large fluctuations in the observed variables.

Initial isotropic and nematic configurations were used for the simulation of linear hard-sphere chain fluids. For partially flexible systems, however, only nematic initial configurations were used, since for these systems simulations starting from an isotropic configuration required very long equilibration periods, typically larger than 5×10^6 Monte Carlo cycles. For linear chains, simulations starting from an isotropic configuration were obtained for a region close to the isotropic-nematic phase transition in order to verify that results in the isotropic and nematic phases are independent of the initial configuration, and to determine the hysteresis at the isotropic-nematic phase transition. Isotropic initial configurations were obtained by placing molecules in the simulation box randomly without a preferred orientation. A nematic configuration was generated by placing molecules in random positions but perfectly aligned on the direction of the largest dimension of the simulation box. In the case of partially flexible molecules, an initial linear molecular configuration was chosen. The initial dimensions of the simulation box were selected in order to ensure that the initial packing fraction of the system is located in either the isotropic or nematic regions. Every simulation run was started from an independent initial configuration in order to avoid correlation between results.

Simulations were performed at constant reduced pressure defined as $P^* = P\, v_{\mathrm{mol}}/k_B T$, where P is pressure, k_B is the Boltzmann constant, T is temperature, and $v_{\mathrm{mol}} = m\pi d^3/6$ is the volume of a molecule made of m beads with diameter d set to unity. The density is expressed dimensionless by the packing fraction $\eta = N v_{\mathrm{mol}}/V$, where N is the number of molecules. The orientational order of the system is measured by the order parameter S_2, which has a value of 0 in an isotropic fluid and a value of 1 for a completely aligned nematic phase. The order parameter S_2 is defined as the ensemble average of the second-order Legendre polynomial,[10] $S_2 = \frac{1}{N}\langle \sum_{i=1}^{N} P_2(\cos\theta_i)\rangle = \frac{1}{N}\langle \sum_{i=1}^{N} (\frac{3}{2}\cos^2\theta_i - \frac{1}{2})\rangle$, where θ_i is the angle between the molecular axis of molecule i and the nematic director **n**. For partially flexible molecules, the molecular axis is defined as the eigenvector corresponding to the smallest eigenvalue of the moment of inertia tensor.[30] In molecular simulations when a nematic phase is formed, molecules do not necessary align across the largest dimension of the simulation box and knowledge *a priori* of the direction of the nematic director is in general not possible. In practice, the orientation of the liquid crystal phase with respect to the laboratory framework is identified with the eigenvectors of the so-called *de Gennes* **Q**-tensor, $\mathbf{Q} = \frac{1}{N}\sum_{i=1}^{N}(\mathbf{q}_i\mathbf{q}_i - \frac{1}{3}\mathbf{I})$,[1] where **q** is a unit vector identifying the direction of the molecular axis with respect to the laboratory frame. In the case that two of the eigenvalues of **Q** are equal, the nematic phase is identified as uniaxial and the nematic director is associated with the eigenvector corresponding to the different eigenvalue, i.e., the largest eigenvalue of **Q**. In the case that all three eigenvalues are the same, the system is found in an isotropic state. For uniaxial phases, $\mathbf{Q} = S(\mathbf{n}\otimes\mathbf{n} - \frac{1}{3}\mathbf{I})$ with corresponding eigenvalues $\lambda_+ = \frac{2}{3}S$ and $\lambda_0 = \lambda_- = -\frac{1}{3}S$, where $S = \sum_{i=1}^{N}(\frac{3}{2}\cos^2\theta - \frac{1}{2})$.[49] The order parameter S_2 can then be estimated as $S_2 = \frac{3}{2}\langle\lambda_+\rangle$. It is important to note that the **Q** tensor is diagonalized for every configuration considered in the ensemble average. An average phase direction can also be obtained by the average $\langle\mathbf{Q}\rangle$, whereby the **Q** tensor is diagonalized only at the end of the simulation run. However, this approach requires that fluctuations in the direction of the nematic director with respect to the laboratory frame are negligible, which is generally not the case and therefore this approach is not implemented here. In this work, the order parameter is obtained from the ensemble average of λ_+ which is calculated every 10^3 Monte Carlo cycles.

The solubility of hard spheres in hard-sphere chain fluids at infinite dilution is described by Henry's law, with dimensionless Henry's law constants defined by[50]

$$\frac{H_2}{\rho_N k_B T} = \exp\left(\frac{\mu_2^{\mathrm{Res},\infty}}{k_B T}\right), \tag{1}$$

where ρ_N is the number density of molecules, and $\mu_2^{\mathrm{Res},\infty}$ is the residual chemical potential of hard spheres in a hard-sphere chain fluid. The residual chemical potential is calculated by the Widom test-particle insertion method,[51] which for Monte Carlo simulations of hard spheres at constant pressure equals[52]

$$\frac{\mu_2^{\mathrm{Res},\infty}}{k_B T} = -\ln\frac{\langle Vp\rangle}{\langle V\rangle}. \tag{2}$$

Here, the parameter p has a value of either 1 for a successful test-particle insertion or 0 for an overlap. A total of 100 test-particle insertions are performed for each configuration sampled every 10^3 Monte Carlo cycles. Since we are interested in the effect of connectivity and molecular anisotropy on the solubility of hard spheres in linear and partially flexible hard-sphere chain fluids, solubility results are expressed as relative Henry's law constants defined by the ratio between Henry's law constants for the solubility of hard spheres in a hard-sphere chain fluid H_2^{HC} to Henry's law constants for the solubility of hard spheres in a hard sphere fluid H_2^{HS} at same packing fraction

$$\frac{H_2^{\mathrm{HC}}}{H_2^{\mathrm{HS}}} = \exp\left(\frac{\mu_{2,\mathrm{HC}}^{\mathrm{Res},\infty}}{\mu_{2,\mathrm{HS}}^{\mathrm{Res},\infty}}\right). \tag{3}$$

The chemical potential of a hard sphere in a hard sphere fluid is calculated from the Boublik-Mansoori-Carnahan-Starling-Leland equation of state.[53] We have verified that this equation is in excellent agreement with our own simulation results for the residual chemical potential of hard spheres in a hard sphere fluid.

III. SIMULATION RESULTS

All results presented in this section are shown in figures. Numerical data for the liquid crystal phase behavior of linear and partially flexible hard-sphere chain fluids is listed in the supplementary material.[59]

A. Linear hard-sphere chain fluids

A systematic study on the liquid crystal phase behavior of linear hard-sphere chain fluids was performed for chain lengths of 7–15 and 20 beads. Previous simulation data for the 7[26,29] and for the 8 and 20[30] linear hard-sphere fluid can be found in the literature. Compared to the literature data, our simulation runs were significantly longer (typically by a factor of 2–10), in particular close to the isotropic-nematic phase transition. In addition, a large number of simulations were performed close to the isotropic-nematic phase transition in order to describe the transition region with high accuracy. The phase behavior of the 7 linear fluid was already determined by Williamson and Jackson[29] and Vega *et al.*[26] Due to the large collection of data existing for this system obtained by two different authors, the 7 linear molecule can be considered as a suitable reference system. Nevertheless, new and more precise simulation data for the 7 linear fluid were obtained. Figure 1 shows the liquid crystal phase behavior of the 7 linear hard-sphere chain fluid from our own results and from the literature data. It can be observed that all simulation data are comparable with slight differences at reduced pressures of 5.0 and higher. From the extensive results obtained in this work, the isotropic-nematic phase transition is found at a reduced pressure of $P^* \sim 3.39$–3.49 at a packing fraction of $\eta^I \sim 0.289$–0.291 for the isotropic phase and of $\eta^N \sim 0.302$–0.303 for the nematic phase. These values lie in between the ranges $P^* \sim 3.15$–3.78, $\eta^I \sim 0.266$–0.303, and $\eta^N \sim 0.285$–0.312 reported by Williamson and Jackson,[29] and it is in agreement with the reduced pressure range $P^* \sim 2.9$–3.7 and packing fractions $\eta^I \approx 0.274$ and $\eta^N \approx 0.308$ reported by Vega *et al.*[26] The large hysteresis at the isotropic-nematic phase transition observed by Williamson and Jackson[29] was not detected here. We suspect that close to the isotropic-nematic phase transition, where fluctuations are large, the simulations results of Williamson and Jackson may either not be well equilibrated or their sampling period was too short (4×10^5 compared to 2×10^6 of our simulations). Nevertheless, a narrow hysteresis of 0.1 in reduced pressure was detected for the 7 linear hard-sphere chain fluid. A phase transition to the smectic-A phase was observed at a reduced pressure $P^* \sim 4.80$–5.00 and $\eta^N \approx 0.359$, $\eta^S \approx 0.380$.

The system size effect of the 7 linear hard-sphere chain fluid was also studied, and results for systems sizes of 216, 350, and 576 molecules are compared in Fig. 2. It can be observed that results for reduced pressure versus packing fraction at the isotropic and nematic regions for all three systems are comparable. However, the precise location of the nematic-smectic phase transition seems to be system size dependent. For the larger 576 molecules system, a first-order phase transition to a smectic-A phase is detected at a reduced pressure between 4.8 and 5.0. On the contrary, for the smaller 350 and 216 molecules systems, partial smectic ordering with no clear defined smectic layers was observed for lower reduced pressure between 4.0 and 5.0. For all three system sizes, smectic-A layers were clearly recognized only at reduced pressures of 5.0 and higher. This system size dependence on the nematic-smectic phase transition was already pointed out by Polson and Frenkel[54] for the nematic to smectic phase transition of hard spherocylinders in the limit of infinite aspect ratio. In their study, the free-energy profile at the nematic-smectic phase transition was calculated for different system sizes (928, 540, and 280 molecules) as a function of smectic ordering. These authors found that a large Gibbs energy

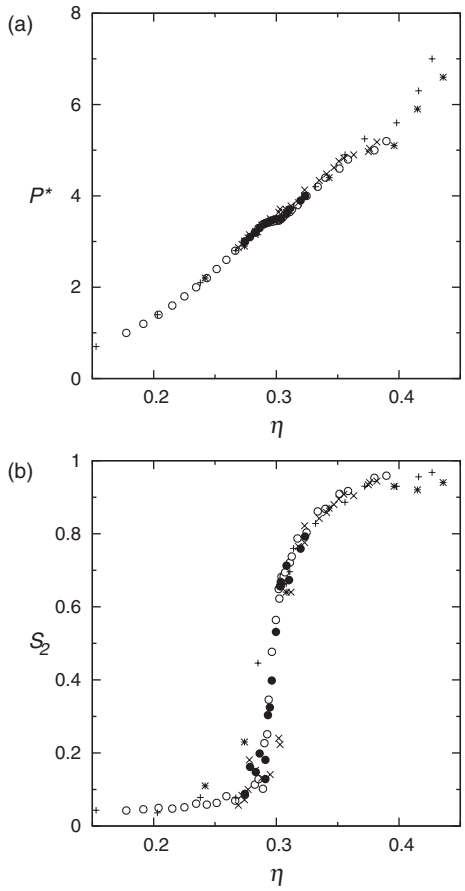

FIG. 1. Liquid crystal phase behavior of the 7 linear hard-sphere chain fluid, reduced pressure P^* (a) and order parameter S_2 (b) as a function of packing fraction η. Results obtained from initial isotropic and nematic configurations are denoted by closed (•) and open circles (○), respectively. Previous data from Williamson and Jackson[29] are denoted by crosses (×) for initial isotropic configurations and by pluses (+) for initial crystal configurations. In addition, results of Vega *et al.*[26] started from a crystal structure are indicated by an asterisk (∗). The size of the symbols is larger than the relative error in the packing fraction (1%–2%) and the relative error in the order parameter (2%–5%) .

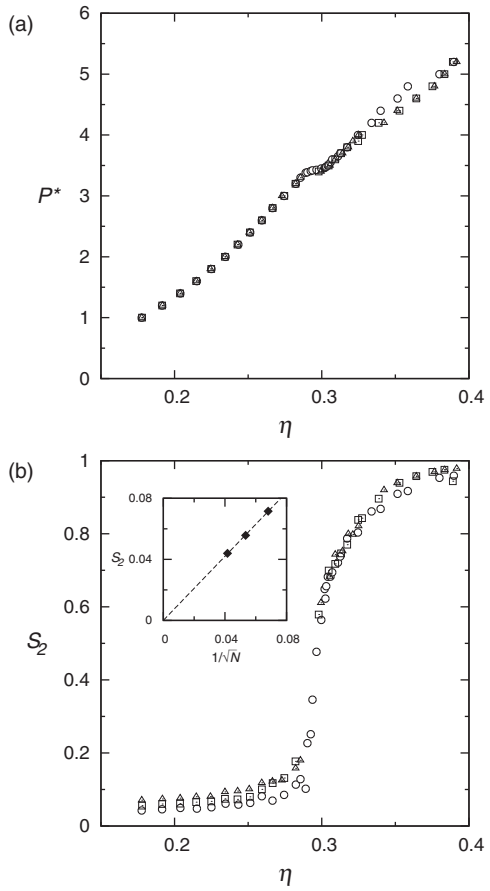

FIG. 2. Finite size effect on reduced pressure P^* (a) and order parameter S_2 (b) for the 7 linear hard-sphere chain fluid as a function of packing fraction η. All results were obtained from initial nematic configurations with system sizes of 216 (△), 350 (□), and 576 (○) molecules. The inset shows the system size dependence of the order parameter for the 7 linear system in the isotropic region at a reduced pressure of $P^* = 1$ and at a packing fraction $\eta \sim 0.178$ for systems sizes of 216, 350, and 576 molecules. In this sub-figure, values are the average of four independent simulation results and the symbol size is larger than one standard deviation. The solid line is a linear fit with $R^2 = 0.999$.

barrier between the nematic and smectic states exists only for the larger system. The Gibbs energy barrier was negligible for the intermediate system size and vanishing for the smaller one. In their work, Polson and Frenkel[54] concluded that, in the thermodynamic limit, the nematic to smectic phase transition of spherocylinders seems to be of first-order for all aspect ratios. Similarly, in our case, a first order nematic-smectic phase transition was observed only for the larger system size of 576 molecules and the partial smectic ordering observed in the smaller systems can be a consequence of a low Gibbs energy barrier caused by the reduced system size.

Another effect of the finite size of the system can be identified in Fig. 2 from the order parameter in the isotropic region. It can be observed that in the isotropic region all three systems show a positive value different than zero for the order parameter, approaching a system-size dependent limiting value as the packing fraction is reduced. The origin of this finite order in the isotropic phase and its corresponding finite order parameter value was described by Eppenga and Frenkel.[10] For isotropic systems of finite size, these authors demonstrated the largest eigenvalue of the **Q**-tensor (from which the order parameter is estimated) deviates from zero by $1/\sqrt{N}$. The inset in Fig. 2(b) shows the relation between order parameter values and system size at same packing fraction. It can be observed that the $1/\sqrt{N}$ dependence is almost exact leading to a vanishing value of the order parameter on the thermodynamic limit.

The phase behavior of the 8, 9, 10, 11, 12, 13, 14, 15, and 20 linear systems is shown in Figs. 3–5. The literature data for the 8 and 20 linear systems from Yethiraj and Fynewever[30] are also included. These authors used a slightly different definition for the order parameter based on the middle eigenvalue of the **Q**-tensor instead of the largest one used here. The middle eigenvalue leads to values of the order parameter that fluctuate around zero in the isotropic phase. Although both definitions are directly related (as shown in Sec. II), we consider the definition based on the largest eigenvalue to be more consistent with the mathematical framework of the **Q**-tensor. Initial isotropic and nematic configurations led to hysteresis in the isotropic-nematic phase transition. The magnitude of the hysteresis showed to be dependent of the packing fraction difference at the isotropic-nematic transition, varying from a difference in reduced pressure of ~0.04 for the 7 linear system to ~0.17 for the 15 linear fluid.

Figures 6 and 7 and Table I summarize the reduced pressure and packing fraction change at the isotropic-nematic transition for all linear systems studied. Reduced transition pressures were calculated at the middle-point of the hysteresis which was estimated by the average of the reduced pressure at coexistence for results starting from an initial isotropic and nematic configurations. Packing fractions were obtained by fitting a third order polynomial on the packing fraction as a function of reduced pressure for each isotropic and nematic branches separately. The isotropic and nematic packing fractions at phase transition were obtained using the previous calculated reduced transition pressures in the fitted equations. Figures 6 and 7 also include the available literature data for the isotropic-nematic phase transition of linear hard-sphere chain fluids. It is observed that the literature data are comparable with our results for the reduced pressure at coexistence but no systematic behavior can be identified from the literature data for the packing fraction difference. From Fig. 6, it can be observed that with increasing chain length, the transition pressure decreases in a continuous manner. On the other hand, from Fig. 7 it can be observed that the packing fraction difference shows a maximum for a chain length of 15 beads. This is a rather surprising result that has not been explicitly reported in the simulation of hard-sphere chain systems before. Bolhuis and Frenkel[20] obtained for spherocylinders the isotropic and nematic densities at coexistence as a function of shape anisotropy L/D by a modified Gibbs-Duhem integration method. From their data, it can be identified that a maximum is reached in the isotropic-nematic density difference at coexistence for a shape anisotropy between 15 and 20. From an Onsager type density functional theory, Fynewever and Yethiraj[55] show a similar behavior of the packing fraction difference for linear hard-sphere chain fluids as a function of chain length, with a maximum at a chain length close to 10. However, neither of these studies mentions the

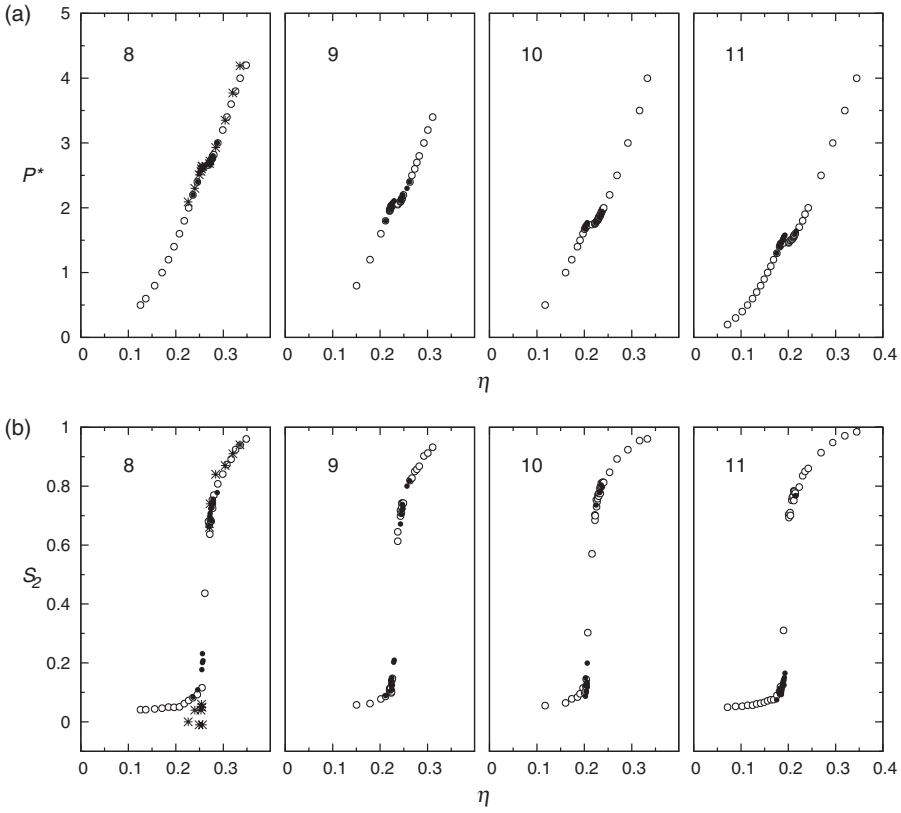

FIG. 3. Liquid crystal phase behavior of linear hard-sphere chain fluids with lengths of 8–11 beads, reduced pressure P^* (a) and order parameter S_2 (b) as a function of packing fraction η. Results obtained from initial isotropic and nematic configurations are denoted by closed (•) and open circles (○), respectively. Previous data from Yethiraj and Fynewever[30] for the 8 linear chain are indicated by an asterisk (∗).

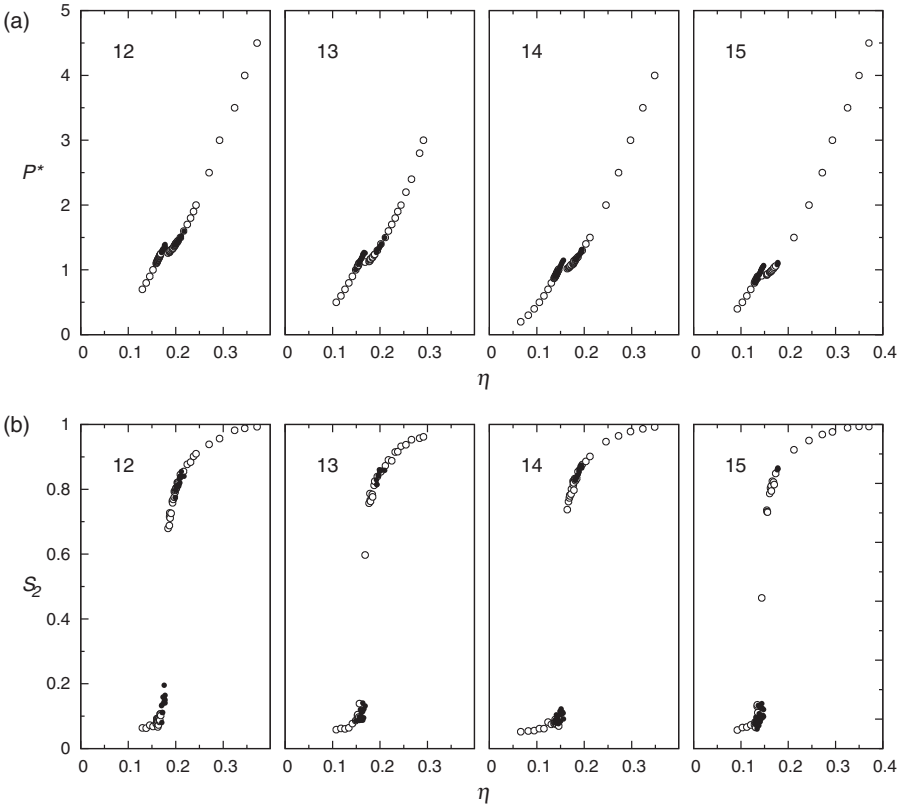

FIG. 4. Liquid crystal phase behavior of linear hard-sphere chain fluids with lengths of 12–15 beads, reduced pressure P^* (a) and order parameter S_2 (b) as a function of packing fraction η. Results obtained from initial isotropic and nematic configurations are denoted by closed (•) and open circles (○), respectively.

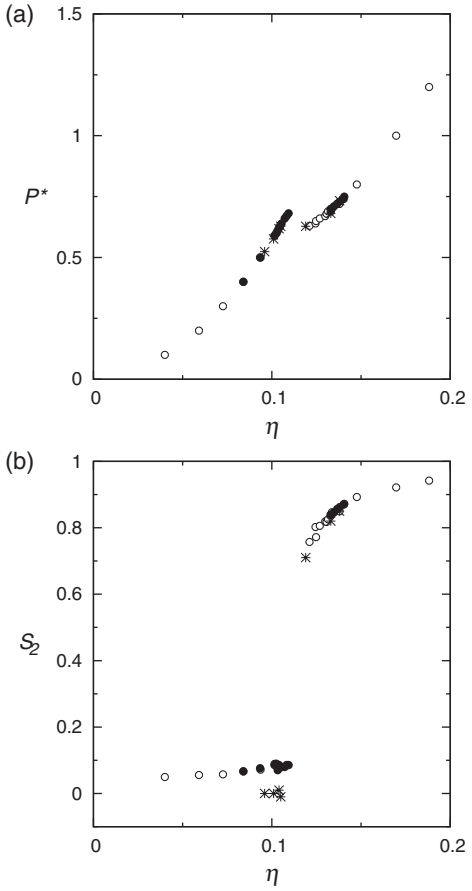

FIG. 5. Liquid crystal phase behavior of linear hard-sphere chain fluids with a length of 20 beads, reduced pressure P^* (a) and order parameter S_2 (b) as a function of packing fraction η. Results obtained from initial isotropic and nematic configurations are denoted by closed (•) and open circles (○), respectively. Previous data from Yethiraj[30] are indicated by an asterisk (∗).

existence of a maximum in the packing fraction difference explicitly.

B. Partially flexible hard-sphere chain fluids

The liquid crystal phase behavior of partially flexible molecules is investigated for different molecular lengths with varying degree of flexibility. Results for this section were obtained from an initial nematic configuration only, since simulations started from an initial isotropic configuration required excessively long equilibration periods. In Fig. 8, the phase behavior of 15-12, 15-13, and 15-14 partially flexible hard-sphere chain fluids is shown. It can be observed that increasing flexibility destabilizes the nematic phase with respect to the isotropic phase, leading to higher transition pressures at higher coexistence packing fractions. The isotropic to nematic phase transition is driven by a difference in the orientational average of the excluded volume between the isotropic and nematic phases.[8] Flexibility reduces this difference,[43] therefore a higher pressure is required in order to induce the transition to the nematic state. Reduced pressures and packing fraction changes at the isotropic-nematic phase transition are summarized in Table II. It can be identified that flexibility increases the transition pressure and reduces the isotropic-

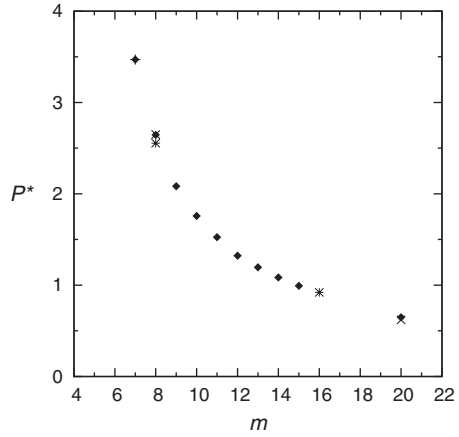

FIG. 6. Transition pressure P^* at the isotropic-nematic coexistence for linear molecules with a length of 7–15 and 20 beads. Previous data from Williamson[29] for the 7 linear (+), Yethiraj[30] for the 8 and 20 linear (×), and from Escobedo and de Pablo[36] for the 8 and 16 linear molecules (∗) are also indicated.

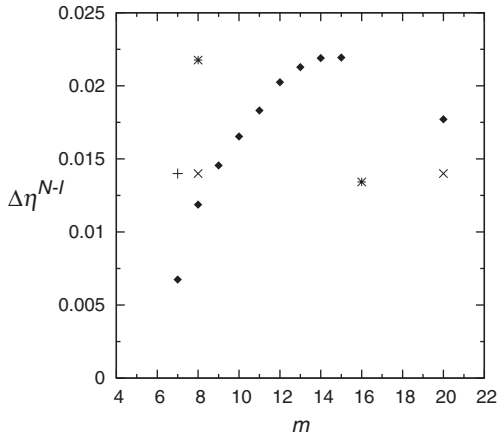

FIG. 7. Packing fraction change $\Delta\eta^{N-I}$ at the isotropic-nematic phase transition for linear molecules with a length of 7–15 and 20 beads. Previous data from Williamson[29] for the 7 linear (+), Yethiraj[30] for the 8 and 20 linear (×), and from Escobedo and de Pablo[36] for the 8 and 16 linear molecules (∗) are also indicated .

TABLE I. Reduced pressure P^*, packing fraction of the isotropic phase η^I, packing fraction of the nematic phase η^N, and packing fraction change at the isotropic-nematic phase transition $\Delta\eta^{N-I}$ for linear molecules with a length of 7–15 and 20 beads.

m	P^*	η^I	η^N	$\Delta\eta^{N-I}$
7	3.47	0.2941	0.3009	0.0068
8	2.65	0.2560	0.2678	0.0118
9	2.08	0.2269	0.2415	0.0146
10	1.76	0.2065	0.2231	0.0166
11	1.53	0.1900	0.2083	0.0183
12	1.32	0.1733	0.1935	0.0202
13	1.20	0.1625	0.1838	0.0213
14	1.09	0.1528	0.1747	0.0219
15	0.99	0.1429	0.1649	0.0220
20	0.65	0.1073	0.1250	0.0177

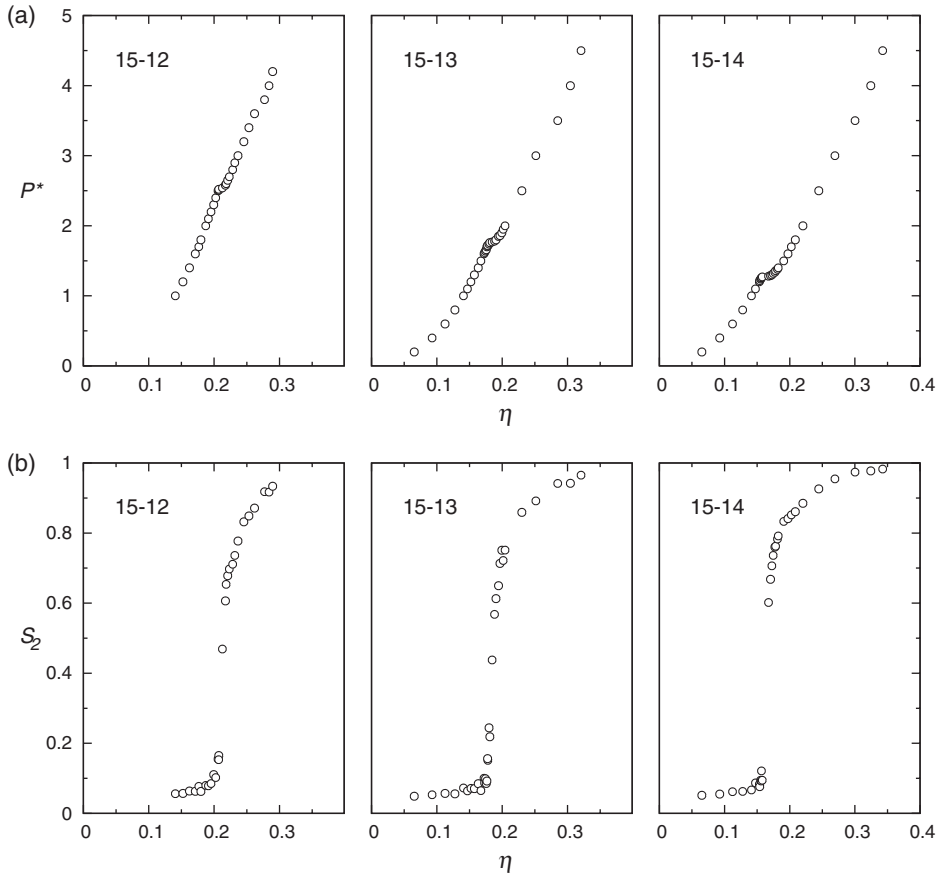

FIG. 8. Liquid crystal phase behavior of 15-12, 15-13, and 15-14 partially flexible hard-sphere chain fluids, reduced pressure P^* (a) and order parameter S_2 (b) as a function of packing fraction η.

nematic packing fraction difference. A transition to a smectic-A phase is identified at a reduced pressure in the range of 3.0–3.5 for the 15-14 and 15-13 fluids and between 3.40 and 3.60 for the 15-12 fluid.

The average end-to-end length in the isotropic and nematic regions for the 15-14, 15-13, and 15-12 partially flexible hard-sphere chain fluids is shown in Fig. 9 as a function of pressure. It can be clearly identified that in the isotropic region the average end-to-end length decreases as pressure increases. This behavior is a consequence of the tendency of molecules to be more entangled at increased packing fractions. On the contrary, a step increase in the average end-to-end length occurs at the isotropic to nematic phase transition. This increased molecular elongation is a result of the orientational ordering in the nematic phase, forcing molecules to stretch along the phase director. Nevertheless, this step-difference in the average end-to-end length at coexistence is relatively small, varying from ∼0.2% for the 15-14 molecule to ∼1% for the 15-12 molecule. In the nematic region, the average end-to-end length increases asymptotically towards the total molecular length with increasing pressure. Although changes in the average end-to-end length are relatively small, Fig. 9 shows that the average molecular configuration of partially flexible hard-sphere molecules varies with reduced pressure (packing fraction) and with molecular ordering, either isotropic and nematic. This change in the average molecular configuration may have an effect on the free volume of the fluid,[43] influencing the solubility of hard spheres in hard-sphere fluids as it will be discussed in Sec. III C.

TABLE II. Reduced pressure P^*, packing fraction of the isotropic phase η^I, packing fraction of the nematic phase η^N, and packing fraction change at the isotropic-nematic phase transition $\Delta\eta^{N-I}$ for 15-14, 15-13, 15-12, 14-13, and 14-12 partially flexible hard-sphere chain fluids.

m	P^*	η^I	η^N	$\Delta\eta^{N-I}$
15-14	1.28	0.1577	0.1740	0.0163
15-13	1.77	0.1788	0.1906	0.0118
15-12	2.54	0.2071	0.2174	0.0103
14-13	1.44	0.1689	0.1841	0.0152
14-12	2.12	0.2034	0.2139	0.0105

Figure 10 shows the liquid crystal phase behavior of the 14-13, 14-12, and 14-10 partially flexible hard-sphere chain fluids. A nematic phase is identified only for the 14-13 and 14-12 fluids. Reduced pressures and packing fraction changes at the isotropic-nematic phase transition for these fluids are specified in Table II. A transition to the smectic-A phase is identified at a reduced pressure in the range of 3.0–3.5 for the 14-13 fluid and 3.5–4.0 for the 14-12 fluid. The more flexible 14-10 fluid does not show a nematic phase, experiencing a continuous transition from the isotropic to the smectic-A phase. The fact that for the 14-10 system the isotropic to smectic phase transition is continuous and is possibly a

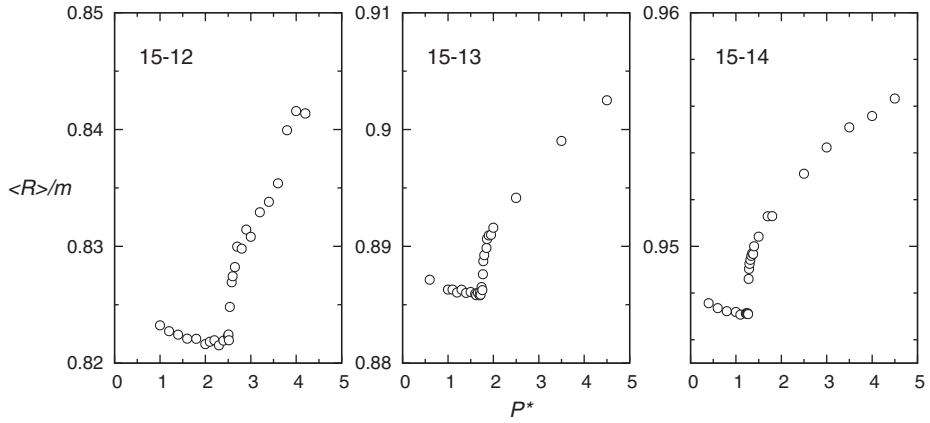

FIG. 9. Average end-to-end length of 15-14, 15-13, 15-12 partially flexible molecules. Results are shown relative to the total chain length m= 15 beads.

consequence of a negligible energy barrier between these phases due to the reduced system size as was already pointed out in Sec. III A for the 7 linear system. However, this premise was not tested here and simulations in larger systems would be required. A clear smectic-A phase could not be recognized for the 14-10 fluid; however, partial smectic-A ordering was observed for reduced pressures of 5.0 and 5.2. A clear smectic-C phase is observed at a reduced pressure of 8.0, but partial smectic-C layering is already identified at reduced pressures between 5.4 and 7.0. Figure 11 shows the phase behavior of the 8-7, 8-6, and 10-8 partially flexible hard-sphere chain fluids. A continuous isotropic to smectic-A phase transition is observed for the 8-7 system in the reduced pressure range of 5.4–5.8 and clear smectic-A layers are identified at reduced pressures of 5.9 and higher. In the 8-6 system, clearly defined smectic-A layers could not be identified; however, partial smectic ordering was observed at a reduced pressure of 14 and higher. For this system, a continuous phase transition from the isotropic to the smectic-A state was observed between reduced pressures of 9.4 and 10.4. Finally, the 10-8

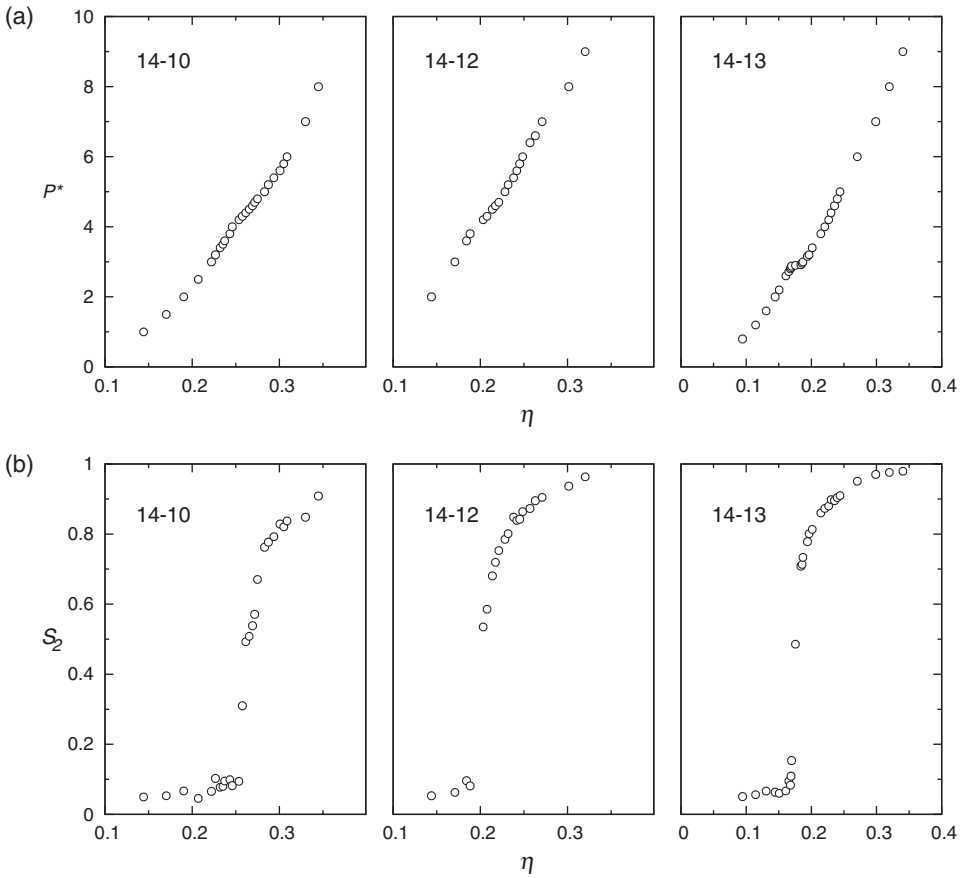

FIG. 10. Liquid crystal phase behavior of 14-10, 14-12, and 14-13 partially flexible hard-sphere chain fluids, reduced pressure P^* (a) and order parameter S_2 (b) as a function of packing fraction η.

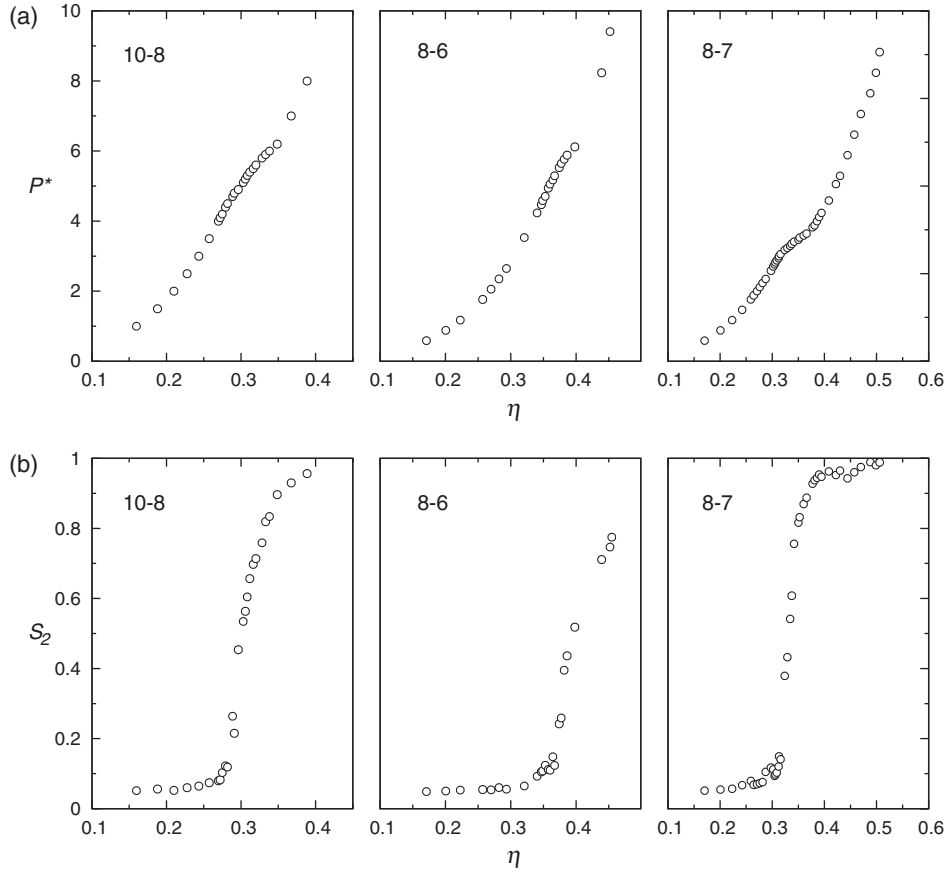

FIG. 11. Liquid crystal phase behavior of 10-8, 8-6, and 8-7 partially flexible hard-sphere chain fluids, reduced pressure P^* (a) and order parameter S_2 (b) as a function of packing fraction η.

fluid shows a continuous phase transition from the isotropic to the smectic-A state between pressures of 4.7 and 5.6 and clear smectic-A layers at pressures of 5.8 and higher.

C. Solubility of hard spheres in hard-sphere chain fluids

The solubility of hard spheres in a hard-sphere chain fluid depends on the available free volume in the fluid, which is in principle determined by the molecular configuration of the hard-sphere chain molecules, packing fraction, and orientation of all molecules in the fluid.[42,43] Here, we investigate the relative importance of these factors by means of relative Henry's law constants defined by Eq. (3).

Figure 12 shows relative Henry's law constants for the solubility of hard spheres in linear hard-sphere chain fluids. From this figure, it can be identified that a linear relationship exists between relative Henry's law constants and packing fraction for all linear fluids. This linearity seems to be independent of liquid crystal ordering and fairly independent of chain length for linear hard-sphere chains of 10 beads and longer. A linear fit calculated from the results for linear hard-sphere chain fluids with a length of 10 and longer is included in Fig. 12.

To verify the independence of solubility with nematic ordering, constant volume Monte Carlo simulations at a constant packing fraction in-between the isotropic-nematic phase transition were performed using an umbrella sampling technique[48] for the order parameter. In these simulations, order parameter values were restricted to ranges of width 0.05 between 0 and 1. The simulation of every order parameter

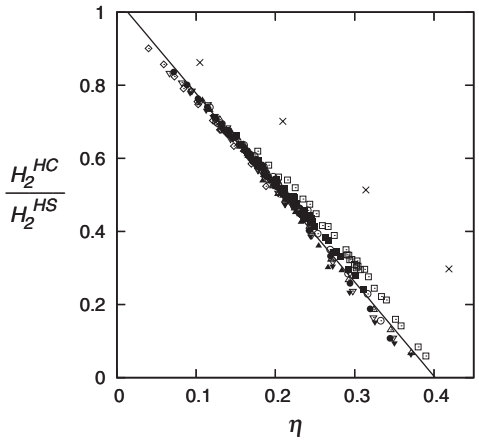

FIG. 12. Relative Henry's law constants for the solubility of hard spheres in linear hard-sphere fluids of length 7 (□), 9 (■), 10 (○), 11 (●), 12 (△), 13 (▲), 14 (▽), 15 (▼), and 20 (◇). The solid line is a linear fit obtained with the data of the 13, 14, 15, and 20 linear hard-sphere chain fluids, with slope −2.580 and intersection 1.036 ($R^2 = 0.991$). Relative Henry's law constants for hard spheres in a hard dumbbell fluid (×) were calculated from the literature data for the chemical potential of hard spheres in a hard dumbbell fluid by Ben-Amotz and Omelyan.[56]

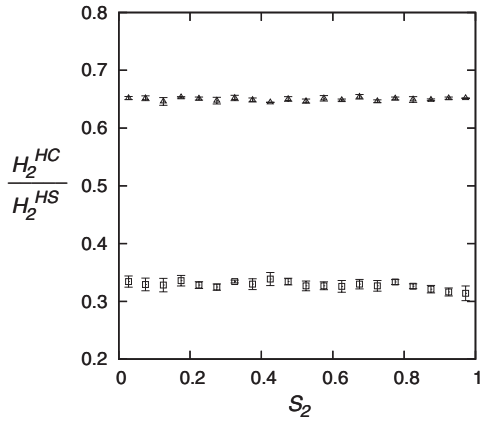

FIG. 13. Relative Henry's law constants as a function of order parameter S_2 for the solubility of hard spheres in a 7 linear hard-sphere fluid at constant packing fraction $\eta = 0.295$ (△) and in a 15 linear hard-sphere fluid at constant packing fraction $\eta = 0.147$ (□).

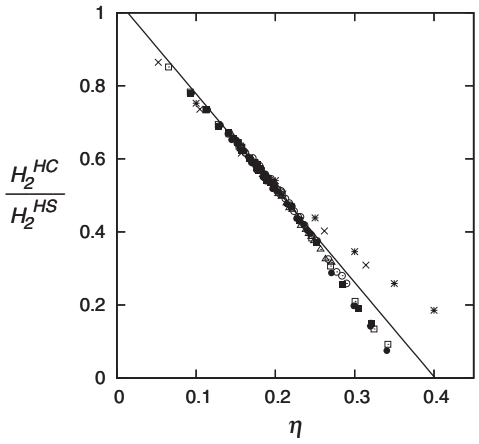

FIG. 14. Relative Henry's law constants for the solubility of hard spheres in 15-14 (□), 15-13 (■), 15-12 (○), 14-13 (●), and 14-12 (△) partially flexible hard-sphere chain fluids. Relative Henry's law constants for hard spheres in a 16 freely jointed hard-sphere fluid were calculated from the data of Escobedo and de Pablo[57] (∗) and from the data of Kumar *et al.*[58] (×).

range was performed separately from an initial nematic configuration which was allowed to freely evolve until a configuration with an order parameter value inside the desired range was obtained. From there on, trial moves that try to change the phase configuration to a new one with an order parameter outside the selected order parameter range were rejected. Figure 13 shows the results for relative Henry's law constants as a function of order parameter for a 7 and 15 linear hard-sphere chain fluid at a constant packing fraction in-between the isotropic-nematic phase transition. From this figure, it can be clearly identified that relative Henry's law constants are independent of the nematic ordering, being constant for a determined value of the packing fraction. This result indicates that at constant packing fraction, the orientation of molecules does not influence the free volume between a hard sphere and a linear hard-sphere chain molecule. Although in the low packing fraction limit, this result is expected due to a negligible interaction between fluid molecules, at finite values of the packing fraction this behavior cannot be known *a priori* due to multibody interactions in the fluid.

Figure 14 shows relative Henry's law constants for the solubility of hard spheres in the nematic forming partially flexible hard-sphere chain fluids. The linear fit obtained for the linear hard-sphere chain fluids is also included in this figure. In contrast to linear hard-sphere chain molecules, the average molecular configuration of partially flexible hard-sphere molecules changes with packing fraction as it was shown in Fig. 9. It can be observed that at packing fractions lower than ∼0.25, the solubility of hard spheres in 15-14, 15-13, 15-12, 14-13, and 14-12 partially flexible hard-sphere chain fluids follows the same linear relationship with packing fraction as for the linear hard-sphere chain fluids. As it is shown in Table II, the isotropic-nematic phase transition of the nematic forming partially flexible hard-sphere chain fluids takes place at packing fractions not higher than 0.2174. This indicates that at packing fractions lower than ∼0.25, the change in the average molecular configuration and the ordering of molecules in the nematic phase do not affect the solubility behavior of hard spheres in partially flexible hard-sphere chain fluids compared to the linear hard-sphere chain fluids. However, this can be a consequence of the relatively short length of the freely jointed part which accounted for a maximal deviation in the end-to-end length lower than 18% compared to the linear case (see Fig. 9). The effect of larger flexibilities is also shown in Fig. 14, relative Henry's law constants calculated from the literature data for the chemical potential of hard spheres in a 16 freely jointed hard-sphere chain fluid[57,58] are also included in this figure. It can be observed that, at low packing fractions, relative Henry's law constants for the partially flexible and fully flexible chain molecules do not appreciably deviate from the linear behavior. At packing fractions higher than ∼0.25, the solubility of hard spheres seems to increase for the nematic forming partially flexible hard-sphere chain fluids and to decrease for the freely jointed hard-sphere chain fluid. Although a solubility increase with flexibility can be expected in the low packing fraction limit from pair excluded volume interactions[43] (not noticeable in Fig. 14), the solubility of hard spheres in partially flexible molecules at high packing fractions cannot be explained from the pair level interaction, since multi-body interactions are relevant.

IV. CONCLUSIONS

An extended description of the liquid crystal phase behavior of linear hard-sphere chain fluids with lengths of 7, 8, 9, 10, 11, 12, 13, 14, 15, and 20 beads was obtained from constant pressure Monte Carlo simulations. For these systems, an accurate description of the isotropic to nematic phase transition was obtained, showing a decrease in the reduced transition pressure with increasing chain length and a maximum in the isotropic to nematic packing fraction change for a chain length of 15 beads. The liquid crystal phase behavior of the partially flexible hard-sphere chain fluids 15-14, 15-13, 15-12, 14-13, 14-12, 14-10, 10-8, 8-7, and 8-6 was also determined. A nematic phase was only observed for the 15-14, 15-13, 15-12, 14-13, 14-12 partially flexible fluids. Other partially flexible fluids experienced a direct transition from the

isotropic to smectic states. In general, flexibility increases the reduced transition pressure and reduces the isotropic-nematic packing fraction difference. The infinite dilution solubility of hard spheres in linear and partially flexible hard-sphere chain fluids was also studied. A linear relationship between relative Henry's law constants and packing fraction was observed for all linear hard-sphere chain fluids. Moreover, this linearity seems to be independent of chain length for linear chains made of 10 beads and longer. The influence of molecular ordering on solubility was also investigated, showing that at constant packing fraction the nematic ordering does not influence the solubility of hard spheres in liquid crystal fluids. Results for the solubility of hard spheres in the nematic forming 15-14, 15-13, 15-12, 14-13, 14-12 partially flexible hard-sphere chain fluids showed that in the isotropic-nematic transition region neither ordering or flexibility affected the linear behavior between relative Henry's law constants and packing fraction obtained from the linear fluids. However, it was observed that at higher packing fractions the solubility of hard spheres seems to increase for the low flexibilities of the nematic forming partially flexible hard-sphere chain fluids and decrease for a freely jointed hard-sphere chain fluid.

ACKNOWLEDGMENTS

This research is supported by the Stichting voor Technische Wetenschappen (Dutch Technology Foundation, STW), applied science division of the Nederlandse organisatie voor Wetenschappelijk Onderzoek (Netherlands Organization for Scientific Research, NWO), and the Technology Program of the Ministry of Economic Affairs. In addition, this work was sponsored by the Stichting Nationale Computerfaciliteiten (National Computing Facilities Foundation, NCF) for the use of supercomputing facilities with financial support from NWO.

[1] P. G. de Gennes, *The Physics of Liquid Crystals* (Oxford University Press, New York, 1974).
[2] G. R. Luckhurst and G. W. Gray, *Molecular Physics of Liquid Crystals* (Academic Press, London, 1979).
[3] G. W. Gray and M. S. Kelly, J. Mater. Chem. **9**, 2037 (1999).
[4] J. Gross and P. J. Jansens, patent application WO2008147181-A1/NL2000654-C2 (4 December 2008).
[5] M. de Groen, T. J. H. Vlugt, and T. W. de Loos, J. Phys. Chem. B **116**, 9101 (2012).
[6] M. de Groen, H. Matsuda, T. J. H. Vlugt, and T. W. de Loos, J. Chem. Thermodyn. **59**, 20 (2013).
[7] G. T. Rochelle, Science **325**, 1652 (2009).
[8] L. Onsager, Ann. N. Y. Acad. Sci. **51**, 627 (1949).
[9] D. Frenkel and R. Eppenga, Phys. Rev. Lett. **49**, 1089 (1982).
[10] R. Eppenga and D. Frenkel, Mol. Phys. **52**, 1303 (1984).
[11] D. Frenkel, B. M. Mulder, and J. P. McTague, Phys. Rev. Lett. **52**, 287 (1984).
[12] D. Frenkel and B. M. Mulder, Mol. Phys. **55**, 1171 (1985).
[13] M. P. Allen, Liq. Cryst. **8**, 499 (1990).
[14] A. Samborski, G. T. Evans, C. P. Mason, and M. P. Allen, Mol. Phys. **81**, 263 (1994).
[15] A. Stroobants, H. N. W. Lekkerkerker, and D. Frenkel, Phys. Rev. A **36**, 2929 (1987).
[16] D. Frenkel, J. Phys. Chem. **92**, 3280 (1988).
[17] A. Stroobants, H. N. W. Lekkerkerker, and D. Frenkel, Phys. Rev. Lett. **57**, 1452 (1986).
[18] D. Frenkel, H. N. W. Lekkerkerker, and A. Stroobants, Nature (London) **332**, 822 (1988).
[19] J. A. C. Veerman and D. Frenkel, Phys. Rev. A **41**, 3237 (1990).
[20] P. Bolhuis and D. Frenkel, J. Chem. Phys. **106**, 666 (1997).
[21] J. A. C. Veerman and D. Frenkel, Phys. Rev. A **45**, 5632 (1992).
[22] D. Frenkel, Mol. Phys. **60**, 1–20 (1987).
[23] M. P. Allen, Philos. Trans. R. Soc. London A **344**, 323 (1993).
[24] C. M. Care and D. J. Cleaver, Rep. Progr. Phys. **68**, 2665 (2005).
[25] M. R. Wilson, Chem. Soc. Rev. **36**, 1881 (2007).
[26] C. Vega, C. McBride, and L. G. MacDowell, J. Chem. Phys. **115**, 4203 (2001).
[27] C. Vega, E. P. A. Paras, and P. A. Monson, J. Chem. Phys. **96**, 9060 (1992).
[28] W. G. Hoover and F. H. Ree, J. Chem. Phys. **49**, 3609 (1968).
[29] D. C. Williamson and G. Jackson, J. Chem. Phys. **108**, 10294 (1998).
[30] A. Yethiraj and H. Fynewever, Mol. Phys. **93**, 693 (1998).
[31] M. Whittle and A. J. Masters, Mol. Phys. **72**, 247 (1991).
[32] M. R. Wilson, Mol. Phys. **81**, 675 (1994).
[33] C. McBride, C. Vega, and L. G. MacDowell, Phys. Rev. E **64**, 011703 (2001).
[34] M. R. Wilson and M. P. Allen, Mol. Phys. **80**, 277 (1993).
[35] C. Vega, C. McBride, and L. G. MacDowell, Phys. Chem. Chem. Phys. **4**, 853 (2002).
[36] F. A. Escobedo and J. J. de Pablo, J. Chem. Phys. **106**, 9858 (1997).
[37] D. S. Chen, G. H. Hsiue, J. D. Schultze, B. Song, and J. Springer, Mol. Cryst. Liq. Cryst. **237**, 85 (1993).
[38] G. H. Hsiue, D. S. Chen, and C. J. Hsieh, Mol. Cryst. Liq. Cryst. **241**, 187 (1994).
[39] M. S. Shannon, J. M. Tedstone, S. P. O. Danielsen, M. S. Hindman, A. C. Irvin, and J. E. Bara, Ind. Eng. Chem. Res. **51**, 5565 (2012).
[40] M. Ramdin, T. W. de Loos, and T. J. H. Vlugt, Ind. Eng. Chem. Res. **51**, 8149 (2012).
[41] C. G. Gray, K. E. Gubbins, and C. G. Joslin, *Theory of Molecular Fluids* (Oxford University Press, Oxford, 2011).
[42] D. C. Williamson and G. Jackson, Mol. Phys. **86**, 819 (1995).
[43] T. van Westen, T. J. H. Vlugt, and J. Gross, J. Chem. Phys. **137**, 044906 (2012).
[44] S. I. Sandler, *Chemical, Biochemichal, and Engineering Thermodynamics*, 4th ed. (John Willey & Sons, Inc., Hoboken, 2006).
[45] D. Frenkel, G. C. A. M. Mooij, and B. Smit, J. Phys.: Condens. Matter **4**, 3053 (1992).
[46] J. I. Siepmann and D. Frenkel, Mol. Phys. **75**, 59 (1992).
[47] J. J. de Pablo, M. Laso, and U. W. Suter, J. Chem. Phys. **96**, 2395 (1992).
[48] D. Frenkel and B. Smit, *Understanding Molecular Simulations*, 2nd ed. (Academic Press, London, 2002).
[49] S. S. Turzi, J. Math. Phys. **52**, 053517 (2011).
[50] K. S. Shing and K. E. Gubbins, Mol. Phys. **46**, 1109 (1982).
[51] B. Widom, J. Chem. Phys. **39**, 2808 (1963).
[52] J. K. Shah and E. J. Maginn, J. Phys. Chem. B **109**, 10395 (2005).
[53] L. E. S. de Souza, A. Stamatopoulou, and D. Ben-Amotz, J. Chem. Phys. **100**, 1456 (1994).
[54] J. M. Polson and D. Frenkel, Phys. Rev. E **56**, R6260–R6263 (1997).
[55] H. Fynewever and A. Yethiraj, J. Chem. Phys. **108**, 1636 (1998).
[56] D. Ben-Amotz and I. P. Omelyan, J. Chem. Phys. **113**, 4349 (2000).
[57] F. A. Escobedo and J. J. de Pablo, J. Chem. Phys. **103**, 2703 (1995).
[58] S. K. Kumar, I. Szleifer, C. K. Hall, and J. M. Wichert, J. Chem. Phys. **104**, 9100 (1996).
[59] See supplementary material at http://dx.doi.org/10.1063/1.4807056 for numerical simulation results (reduced pressure P^*, packing fraction η, and order parameter S_2) for the phase behavior of hard-sphere linear chain fluids made of 7, 8, 9, 10, 11, 12, 13, 14, 15, and 20 beads, and for 15-14, 15-13, 15-12, 14-13, 14-12, 14-10, 10-8, 8-7, 8-6 partially flexible hard-sphere chain fluids.